HHS Public Access

Author manuscript

Chemistry. Author manuscript; available in PMC 2024 February 21.

Published in final edited form as:

Chemistry. 2023 February 21; 29(11): e202203588. doi:10.1002/chem.202203588.

Gated, Selective Anion Exchange in Functionalized Self-Assembled Cage Complexes

Bryce da Camara,

Noa Bar Ziv,

Veronica Carta,

Gabriela A. Mota Orozco,

Hoi-Ting Wu,

Ryan R. Julian,

Richard J. Hooley

Department of Chemistry and the UCR Center for Catalysis, University of California - Riverside, Riverside, CA, 92521, U.S.A.

Abstract

Appending functional groups to the exterior of Zn_4L_4 self-assembled cages allows gated control of anion binding. While the unfunctionalized cages contain aryl groups in the ligand that can freely rotate, attaching inert functional groups creates a “doorstop”, preventing rotation and slowing the guest exchange rate, even though the interiors of the host cavities are identically structured. The effects on anion exchange are subtle and depend on multiple factors, including anion size, the nature of the leaving anion, and the electron-withdrawing ability and steric bulk of the pendant groups. Multiple exchange mechanisms occur, and the nature of the external groups controls associative and dissociative exchange processes: these bulky groups affect both anion egress and ingress, introducing an extra layer of selectivity to the exchange. Small changes can have large effects: affinities for anions as similar as PF_6^- and SbF_6^- can vary by as much as 400-fold between identically sized cavities.

Graphical Abstract

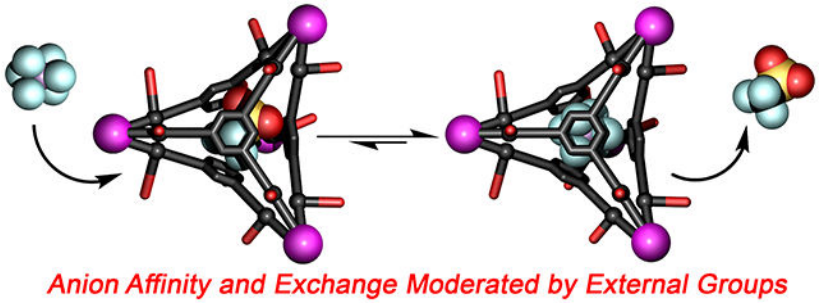

richard.hooley@ucr.edu. @RichardJHooley.

Supporting information for this article is given via a link at the end of the document.

Appending functional groups to the exterior of Zn_4L_4 self-assembled cages allows gated control of anion binding. The external groups act as a “doorstop”, preventing ligand rotation and slowing the guest exchange rate. Bulky groups affect both anion egress and ingress, introducing an extra layer of selectivity to the exchange. Small changes can have large effects: affinities for anions as similar as PF_6^- and SbF_6^- can vary by as much as 400-fold between identically sized cavities.

Keywords

Supramolecular chemistry; Self-assembly; Coordination Chemistry; Anion binding; Molecular recognition

Introduction

Substrate molecular recognition in proteins is exquisitely controlled by a number of small weak forces: multiple small changes in structure maximize affinity for substrate, and modulate the in/out exchange rate.[1] Synthetic receptors, on the other hand, tend to be rigid and exploit preorganization for maximal binding affinity.[2] While there are numerous methods known for controlling guest entry,[3] most examples of flexible entry portals are seen with hydrogen-bonded capsules, where individual walls can open and close by breaking a subset of the H-bonds, retaining the assembled structure while allowing guest ingress and egress.[4] Bowl-shaped or toroidal macrocycles generally do not require flexible entry portals (as they are open-ended), but there are some examples of guest exchange moderated by wall motion in deep, self-folding cavitands.[5] Self-assembled metal-ligand cage complexes are held together by stronger individual interactions, however, which limits flexibility. Many hosts show relatively large “panel gaps” that allow easy and rapid guest ingress.[6] More enclosed cage hosts often require distortion of one or more ligand walls to allow an opening,[7] have switchable entry portals for controlled exchange,[8] or use reversible ligand dissociation for guest control.[9] External agents can also be added to “cap” the open portals.[10] The vast majority of self-assembled metal-ligand cage complexes use symmetrical, unfunctionalized ligands to ensure reliable assembly, so the introduction of pendant groups[11] to these ligands to control guest entry is quite rare. Functional groups have been added to the edges of cage ligands,[12] but their effects on guest binding are either minimal, or their effects have not been studied in detail.[13] Here we describe the effect of introducing flexible pendant groups into a series of M_4L_4 tetrahedra on the selective molecular recognition of suitably sized anions, and their gating effect on the binding kinetics.

The cage structures used are shown in Figure 1, and consist of tripodal tris-amine ligands that are capable of assembly into M_4L_4 tetrahedra[14] upon multicomponent assembly with Zn^{2+} or Fe^{2+} salts and 2-formylpyridine (PyCHO, Figure 1). Cages **1–3** use electron poor triazine cores, whereas cages **4** and **5** contains an electron rich phenyl core. The unfunctionalized cages are known: triazine ligand **L1** has been assembled into the Fe_4L_4 tetrahedron **Fe-1**,[15] and the unfunctionalized phenyl ligand **L5** has been used to make both Fe_4L_4[15] and Zn_4L_4[16] cages **Fe/Zn-5**, all of which can bind suitably sized anions such as ClO_4^- or OTf^- in the cavity. These tripodal ligands form a tightly enclosed cage, with only

small spaces between the panels. In each case, the aryl arms can rotate about the central axis, acting as a "revolving door"[5a] that enables guest ingress. Our question is whether the anion binding selectivity and ingress/egress mechanism can be altered by attaching inert functional groups to the ligands, acting as a "doorstop" for the rotation. Cages **2–4** can therefore provide a unique insight into the effect of gating functional groups on the kinetics of anion recognition.

Results and Discussion

The first question is whether the functionalized cages could be cleanly formed. Ligands **L1-L3** were synthesized in 3 steps from 1,3,5-trichlorotriazine and the corresponding nitrophenol in good yield, and **L4** was formed *via* an analogous method to the known **L5**[15,16] (see Supporting Information for synthesis and characterization). The ether connections between the core triazine/aryl ring of ligands **L2-L4** and the three aniline arm groups allow rapid rotation of the functionalized anilines around the C-O-C axis, and as such, the R groups on the pendant aryl rings of **L2-L4** could theoretically adopt multiple different conformations after assembly. To test this, the ligands were assembled into the corresponding Zn_4L_4 cage complexes by heating with Zn^{2+} salts and 2-formylpyridine in CH_3CN at 50 °C for 16 h. The structures of cages **1–4** (defined as the Zn_4L_4 cages of **L1-L4**) with various counterions were analyzed by ^1H, ^{13}C and ^{19}F NMR, as well as ESI-MS, and compared to the known **5**. COSY and NOESY NMR were used in certain cases for additional structural confirmation and peak assignment.

Successful assembly with ligands **L1-L4** was dependent on the corresponding counterion (as had been observed by Kruger[15] for **L1**). Our "standard" method used $Zn(OTf)_2$, which allowed successful formation of all cages **1–4•OTf**. ^{19}F NMR and ESI-MS analysis confirmed the presence of a bound OTf^- anion in each case: importantly, no peaks for the unoccupied cages were observed in the ESI-MS spectra, suggesting that the counterion has a templating effect on the synthesis (see Figures S32–33). While ligand **L1** could be assembled with a wide range of Fe^{2+} and Zn^{2+} salts, the functionalized ligands **L2-L4** were more picky. The "unoccupied" cage **1** could be formed with $Zn(NTf_2)_2$,[16] but using $Zn(NTf_2)_2$ with the functionalized ligands **L2-L4** did not give any evidence of cage formation: the "empty" cages **2–4** could not be accessed. We were not able to obtain single crystals of the Zn cages **2–4** that diffracted well enough for publication, but we were able to obtain an X-ray structure of the structurally analogous Fe cage **Fe-4•SbF_6** (CCDC 2213841; see Supporting Information and Figure 2a). Minimized structures of **Zn-2•SbF_6** and **Zn-3•SbF_6** are shown in the Supporting Information, illustrating their strong structural similarity to **Fe-4•SbF_6**, and the known structures of **Fe-1•OTf**[15] and **Zn-5•SbF_6**.[16] The NMR, SCXRD and MS analysis shows that cages **2–4•OTf** form tetrahedrally symmetric Zn_4L_4 complexes (Figure 1), with one OTf^- anion bound in the cavity and the twelve R groups (Me or CO_2Me respectively) all oriented externally: the cavity sizes for cages **1–5** are all essentially identical.

The similarity in structure between cages **1–3** enables an analysis of the effects of small gating groups on anion binding and exchange properties. For consistency, and as only cage **1** could be synthesized with an "empty" cavity, we used the three $Zn(OTf)_2$ cages

1–3•OTf to analyze the effect of the methyl and carboxymethyl substituents on the anion binding properties. Cages **1–3•OTf** were treated with a variety of non-coordinating anions in CD_3CN solution, and their exchange with bound OTf^- was monitored. The anions tested ranged from "too large" (NTf_2^- and BPh_4^-), to "too small" (BF_4^-), to "just right" (ClO_4^-, PF_6^-, AsF_6^-, SbF_6^-). The templating OTf^- anions bind strongly in cages **1–3•OTf** (Nitschke reported K_a (OTf^-) = 3.1 ×10^4 M^{-1} in **Zn-5•NTf$_2$**[16]), and no displacement of OTf^- could be observed upon treatment with NTf_2^-, BPh_4^- or BF_4^-. Interestingly, BPh_4^- did cause significant shifts in the pyridyl signals in cages **1–2•OTf** (see Figure S-57), as it binds to the exterior of the cage (as has been seen for other M_xL_y cages).[17] However, anions such as ClO_4^-, PF_6^-, AsF_6^-, SbF_6^- are suitably sized for internal binding, and effected displacement of OTf^- from the cavity of **1–3•OTf**. The surprising observation was the rate of exchange, which was extremely slow, especially for functionalized cages **2,3•OTf**: in these cases, exchange requires up to *days* of heating at 50 °C. This is in contrast to the unfunctionalized cages **Fe-1**, **Fe-5** and **Zn-5**, which undergo anion displacement in seconds (**Fe-5**[15] and **Zn-5**[16]) or require moderate heating for a few hours (**Fe-1**[15]).

The exchange process can be monitored by changes in the ^1H NMR spectra: as might be expected, observable changes in the shift of the imine protons H_e or the internal C-H arene proton H_f occur when the internal anion is replaced (see Figures S58–61 for NMR data). For example, after 8 h at 50 °C, complete exchange of AsF_6^- is seen with **1•OTf**, whereas only 65 % exchange is seen with **2•OTf**, and <15 % with **3•OTf**. Even after 60 h heating with an excess of competitive anion, equilibrium is not reached with **3•OTf**. This data is mirrored with the other anions: exchange of PF_6^- and SbF_6^- occurs on the same general timescale as AsF_6^-, but the rates vary significantly between the three cages **1–3•OTf**. The exchange rate profiles were analyzed with pseudo-first order plots under low conversion, and the initial rates of exchange were calculated. Figure 3b shows the exchange rate profiles upon adding 25 mM PF_6^-, AsF_6^- and SbF_6^- to 1 mM cages **1–3•OTf** (i.e. 8 mM total OTf^-, for full data, see Supporting Information) and heating at 50 °C. The fastest rate was seen with PF_6^- and **1•OTf**, with an initial rate of exchange of 0.10 mM/h. In this case, the rate was dependent on anion size, with the smaller PF_6^- (calculated volume[18] = 98 $Å^3$) exchanging faster than the larger AsF_6^- (108 $Å^3$) or SbF_6^- (118 $Å^3$) anions. Exchange in the gated methyl cage **2•OTf** was slower (~0.05 mM/h) and less dependent on anion size, and ester cage **3•OTf** showed an even slower anion exchange (0.022 mM/h, almost 5-fold slower than in **1•OTf**) and no dependence on anion size.

An important consideration in analyzing the in/out rate is the overall binding constant: if the affinity of the added ions is not high enough, obviously 100% expulsion of the OTf- ion will not be achieved. As such, the binding affinity relative to that of OTf^- (K_{rel}) for BF_4^-, PF_6^-, AsF_6^- and SbF_6^- in cages **1–3** was determined, and is shown in Table 1. As the corresponding NTf_2^- cages for the functionalized ligands could not be formed, all affinities are quoted relative to that of OTf^- (see Supporting Information for K_{rel} calculations). As such, the samples were heated until full equilibrium was observed, up to 2 weeks at 50 °C. After 3 days cage **1•OTf** reached consistent equilibrium, but the exchange rate for and **2•OTf** and **3•OTf** was so slow that equilibrium was not reached for up to two weeks. As the cage system was beginning to show signs of decomposition at this time, a "lower limit" of

relative affinity between anions and **2/3•OTf** was established. The true K_{rel} is likely slightly higher than that in Table 1, but the stated data is the best estimate possible. In each case, BF_4^- bound significantly more weakly than OTf^-, and no OTf^- exchange could be seen. Changes in the external group caused some unusual differences in target affinity for the other anions, though: in unfunctionalized cage **1**, PF_6^-, AsF_6^- and SbF_6^- all bound more strongly than OTf^-, but there was essentially no difference in the affinity of each of these three anions for cage **1**. The affinity of SbF_6^- in **1** is an estimate, as the shifts in ^1H NMR peaks are too small to analyze, and the integration of bound SbF_6^- in the ^{19}F spectrum is complicated by the complex coupling pattern. In contrast, for cages **2** and **3**, AsF_6^- showed the greatest affinity, and the differences between PF_6^-, AsF_6^- and SbF_6^- were much more pronounced. For example, AsF_6^- is the best guest for cages **2** and **3**, showing 58-fold stronger binding than OTf^- in **2**. It binds 38-fold more strongly in cage **3** than OTf^-, and 16-fold more strongly than PF_6^-, despite the similarities in size.

These results illustrate that addition of “inert” functional groups to the exterior of the Zn_4L_4 scaffold can have large effects on the binding affinity and exchange rate of added anions, despite the cavity sizes being almost identical. Differences between **1•OTf** and **2/3•OTf** are perhaps to be expected – the phenyl groups in **1** can rotate in the assembly, whereas the equivalents in **2/3** are locked. Importantly, there is no difference in cavity size between **2•OTf** and **3•OTf**, as the groups are oriented externally, but there are marked differences in guest affinity. Also, the factors that govern exchange rate cannot be the same as those that govern affinity, as the exchange rate does not directly correlate with binding affinity. Looking at the PF_6^-, AsF_6^- and SbF_6^- subset, the fastest exchange rate with cage **2•OTf** is shown by SbF_6^-, but the strongest affinity anion is AsF_6^-. The in/out rate for cage **1•OTf** correlates strongly with anion size, but this is not observed for **3•OTf**, where the exchange rates are almost identical, yet the relative binding affinity varies 10-fold between PF_6^- and SbF_6^-.

An additional factor to consider is that the anion exchange rate is dependent on the presence of a bound anion in the cavity. When PF_6^- anions are added to **1•NTf$_2$** (the only “empty” variant that can be accessed amongst **1–3**), anion binding is very rapid: complete incorporation of anion is observed in <3 mins at ambient temperature, in contrast to the hours required to expunge OTf^- ions from the cavities of **1–3•OTf**. This leads to the question of whether the nature of the “leaving group” anion is an important factor in the exchange rate. To test this, **2•SbF$_6$** and **3•SbF$_6$** were synthesized by heating **2•OTf** and **3•OTf** with a large excess of $NaSbF_6$ overnight, followed by isolation of the SbF_6-bound cages. These complexes were then treated with $NaAsF_6$ (which binds more strongly in both cages **2** and **3** than SbF_6^-), and the rate of AsF_6^- incorporation compared to that with the OTf- bound cages. As can be seen in Figure 4c, changing the leaving anion has significant implications to the exchange rate. The more strongly bound SbF_6^- is expunged far more slowly in each case than OTf^-: 3-fold with **2**, and 6-fold with **3** (see Supporting Information for initial rate plots).

This behavior indicates that both the incoming and leaving guests have an effect on the rate, as well as the cage structure. There are two possible mechanisms, illustrated in Figure 4. An “S_N2-like” associative process is possible, with the leaving anion directly replaced

by incoming guest. Alternatively, a dissociative "S_N1-like" mechanism can occur whereby the bound anion leaves, initially replaced by CH_3CN solvent, followed by a rapid entry of the second anion. The rapid ingress of anions to the "empty" cage Zn-**1•NTf$_2$** and lack of any observable "free" **2** or **3** during the exchange suggest that OTf^- egress is rate-determining in the dissociative mechanism. To determine whether this was the dominant mechanism, the concentration of incoming anion was varied (PF_6^-, AsF_6^- and SbF_6^- were each tested at 8, 25 and 75 mM with 0.8 mM cages **1–3•OTf** at 50 °C) and the initial rate analysis repeated to determine the order of the process with respect to incoming anion (see Figures S-70–75, Table S-3). In each case, the exchange rate was dependent on the concentration of incoming anion. However, the processes were not first order, but varied in order from 0.2 – 0.7, indicating that both processes occur and the amount of associative "S_N2-like" displacement is dependent on the nature of the incoming anion and the cage. Counterintuitively, the greatest dependence on [incoming anion] was seen with the largest anion SbF_6^-. The obvious theory would be that the smaller anion PF_6^- would more easily fit through the small panel gaps in **2–3•OTf** and would favor the associative process, but the observed order for PF_6^- in **2•OTf** was 0.2, whereas that of SbF_6 was 0.7. This data, as well as the rate data shown in Figure 3 at a constant [anion] shows that the factors controlling the exchange rate in **1–3** are quite complex: multiple mechanisms are occurring, all of which can be affected by the external groups.

Finally, the exchange behavior of the phloroglucinol cages **4** and **5** is markedly different. The more electron rich phenyl walls vastly increase the anion binding exchange rate, compared to **1–3** (this was also noted by Kruger,[15] when comparing **Fe-1** and **Fe-5**). Upon addition of either PF_6^-, AsF_6^- and SbF_6^- ions to **Zn-4•OTf**, complete equilibration between the added and expunged anion occurred in seconds, rather than the days/weeks needed for **Zn-(1–3)•OTf**. The affinity data for phloroglucinol cage **4** was also unusual: whereas cage **5** showed relatively similar affinities for similarly sized anions, with identical affinities for OTf^- and AsF_6^- and only a 6-fold greater affinity for SbF_6,[16] ester cage **4** shows significant selectivity for the larger SbF_6^- (K_{rel} = 44), whereas AsF_6^- and PF_6^- bind *more weakly* than OTf^-. In this case, the selectivity for SbF_6^- over AsF_6^- is greater than 100-fold.

The NMR data and the crystal structure of **Fe-4•SbF$_6$** give some insights into the recognition. Both the central ring in the ligand (either electron-poor triazine or electron-rich arene) and the C-H groups of the pendant phenyl arms are in close proximity to the bound guest, and so both anion-pi and C-H anion interactions are present in the host:guest complex (as well as charge considerations and desolvation effects, but those are all constant between the different cages). While cavity sizes in Zn-**1–5** are extremely similar, calculated to be ~145 $Å^3$,[16],[18] the cages are slightly flexible, so can adapt to the size and shape of the guest. As well as simple space-filling factors, the anion affinity is controlled by interactions with some of the 4 central ring faces (a close-up image is shown in Figure 5c), but also the edge C-H bonds of the pendant arenes. In **1** and **5**, these rotate, whereas in **2–4**, they are fixed: it is not clear whether the fixed orientation (and permanent introversion of the C-H groups on the arene ring) shrinks the effective cavity size or provides favorable C-H–anion interactions between host and guest. The affinities do not follow Rebek's 55% rule:[19]

this is to be expected, as that "rule" was determined for neutral hydrocarbon guests in neutral capsules, and anion binding is driven by electrostatic interactions. For example, the space occupancy can be calculated for AsF_6^- as 74%, using the cavity and anion volumes described above. The most obvious explanation is that AsF_6^- provides that best size and shape match for the cavities, hence the higher affinity in most cases. This leaves a single outlier: the significantly higher affinity for SbF_6^- in cage **4**. The variable in this case is the presence of a phenyl core, as opposed to the triazine in **1–3**. The selectivity for the larger SbF_6^- must therefore be due to anion-pi interactions between the more electron rich arene, and the softer, more diffuse SbF_6^- ion. This selectivity is also seen in **5**,[16] albeit to a much lesser extent. The strong selectivity shown by **4** is likely a combination of interactions between guest and the arene, as well as enhanced CH-anion interactions in **4**, due to the external electron-withdrawing ester group.

When considering the *exchange rate*, simply considering the cavity size and guest shape-fitting is not sufficient. The first question is whether the cage remains intact during the exchange process. The variable effects of anion size on the exchange rate, and differences between **1–3** and **4–5** suggest that ligand dissociation from the Zn centers,[3],[4a],[8b],[9] "opening" the cage, is not prevalent. We have no evidence that the ligands dissociate from the complex over the time period monitored, and the fact that the cage is stable for weeks at 50 °C in wet CD_3CN suggests that process is not occurring. The mechanism cannot be fully ruled out, but would not explain the large exchange rates differences between cages of essentially identical stability. The likely exchange mechanism is therefore that the ligand-metal bonds remain intact, and the walls distort to allow guest ingress/egress.[7b]

One dominant factor in the exchange rate is the central ring, as noted by Kruger:[15] anion exchange occurs in seconds in **4**/**5**, as opposed to days or even weeks in **1–3**. The more favorable anion-pi interactions with the triazine ring cause significant slowing of the in/out exchange rate. Among the highly similar cages **1–3**, which only differ in the nature of the external group, the story becomes far more complex. Two mechanisms are present, associative and dissociative, the relative proportions determined by the nature of cage and incoming anion. The freely rotating groups in **1•OTf** confer a faster in/out exchange rate on the guests. When the pendant aryl groups are "locked" by the presence of external $-CH_3$ or $-CO_2Me$ groups, the exchange rate drops, up to 5-fold. Increasing the size of the group adds a second "blocking" layer of hindrance to the cage exterior, which limits access of incoming anions to the cage walls: Figure 5a and 5b show CPK representations of two SCXRD structures of cage-SbF_6 complexes, Nitschke's structure of the unfunctionalized **Zn-5•SbF$_6$**,[16] and our **Fe-5•SbF$_6$**, which illustrates the blocking nature of the $-CO_2Me$ groups nicely.

The extra bulk obscures the entry portals, which affects the exit rate of the bound anion, as well as the entry rate of the incoming anion, hence the varying dependence of the reaction rate on both incoming and outgoing anion, as well as the varying order of the process. While the variations in order are small, some trends can (cautiously) be predicted: the more hindered cage **3•OTf** shows a slightly increased order dependence on nucleophile than **2•OTf**, suggesting that OTf^- egress is slowed, increasing the proportion of "S_N2-like" associative mechanism, albeit only slightly. This also explains the rate dependence of cages

1–3•OTf on anion type: for the unhindered cage **1•OTf**, the rate depends on incoming anion size, as the smaller anions can fit through the portals more easily. This effect is not seen for "locked" cage **3•OTf** (and only very slightly for **2•OTf**): adding size to the anion no longer reduces the entry rate. But for cages **2–3•OTf**, the slowed exit rate of the OTf^- anion (due to the blocking groups) increases the proportion of S_N2-like associative exchange. This leaves the question of why SbF_6^- favors an associative exchange mechanism most (and most obviously in the ester cage **3**), which is less clear. Perhaps the more diffuse negative charge in the larger anion is less repelled by the external groups upon entry (especially the electron-rich CO_2Me groups), but this is merely speculation. What is clear is that small changes in the structure of the exterior of self-assembled cage complexes can have unexpected, and in some cases large effects on the affinity and exchange rate of bound guests, despite almost identical interior cavity shapes and sizes.

Conclusion

In conclusion, we have shown that appending functional groups to the exterior of M_4L_4 tetrahedral self-assembled cages allows gated control of anion binding (both affinity and exchange rate) in the cavity. The effects of the pendant external groups are subtle and depend on multiple different factors, including anion size, the nature of the leaving anion, and the electron-withdrawing ability and steric bulk of the pendant groups. Multiple exchange mechanisms occur, and the nature of the external groups controls the proportion of associative and dissociative exchange processes occurring: these bulky groups affect both anion egress and ingress, introducing an extra layer of selectivity to the exchange. These properties are reminiscent of the subtle effects that control gating and selective molecular recognition in enzyme active sites, not simply a shape-filling "lock and key" mechanism: this concept is important in the design of size- and shape selective catalytic hosts and biomimetic systems.

Data Availability Statement

The data that support the findings of this study are available in the supplementary material of this article. Deposition Number(s) 2213841 (for Fe-4•SbF6) contains the supplementary crystallographic data for this paper. These data are provided free of charge by the joint Cambridge Crystallographic Data Centre and Fachinformationszentrum Karlsruhe Access Structures service.

Supplementary Material

Refer to Web version on PubMed Central for supplementary material.

Acknowledgements

The authors would like to thank Prof. Gregory J. O. Beran for assistance with Gaussian calculations and the National Science Foundation (CHE-2002619 to R. J. H.; CHE-1904577 to R. R. J.; CHE-1919677 for purchase of a diffractometer) for funding. G. A. M. O. was supported by a grant from the National Institutes of Health (T34GM062756).

References

[1]. a)Sullivan SM, Holyoak T, Proc. Natl. Acad. Sci. U. S. A 2008, 105, 13829–13834; [PubMed: 18772387] b)Sullivan SM, Holyoak T, Biochemistry. 2007, 46, 10078–10088. [PubMed: 17685635]

[2]. a)Young NJ, Hay BP, Chem. Commun 2013, 49, 1354–1379;b)Chakrabarty R, Mukherjee PS, Stang PJ, Chem. Rev 2011, 111, 6810–6918; [PubMed: 21863792] c)Rizzuto FJ, von Krbek LKS, Nitschke JR, Nat. Rev. Chem 2019, 3, 204–222;d)Saalfrank RW, Maid H, Scheurer A, Angew. Chem., Int. Ed 2008, 47, 8794–8824;Angew. Chem 2008, 120, 8924–8956;e)Cook TR, Stang PJ, Chem. Rev 2015, 115, 7001–7045; [PubMed: 25813093] f)Ward MD, Raithby PR, Chem. Soc. Rev 2013, 42, 1619–1636. [PubMed: 22797247]

[3]. Akine S, Sakata Y, Chem. Lett 2020, 49, 428–441.

[4]. a)Craig SL, Lin S, Chen J, Rebek J Jr., J. Am. Chem. Soc 2002, 124, 8780–8781; [PubMed: 12137515] b)Santamaria J, Martin T, Hilmersson G, Craig SL, Rebek J Jr., Proc. Natl. Acad. Sci. U.S.A 1999, 96, 8344–8347; [PubMed: 10411877] c)Gottschalk T, Jaun B, Diederich F, Angew. Chem., Int. Ed 2007, 46, 260–264;Angew. Chem 2007, 119, 264–268.

[5]. a)Hooley RJ, van Anda HJ, Rebek J Jr., J. Am. Chem. Soc, 2006, 128, 3894–3895; [PubMed: 16551081] b)Hooley RJ, van Anda HJ, Rebek J Jr., J. Am. Chem. Soc, 2007, 129, 13464–13473. [PubMed: 17927175]

[6]. a)Northrop BH, Zheng Y-R, Chi K-W, Stang PJ, Acc. Chem. Res 2009, 42, 1554–1563; [PubMed: 19555073] b)Fujita M, Tominaga M, Hori A, Therrien B, Acc. Chem. Res 2005, 38, 371–380.

[7]. a)Caulder DL, Raymond KN, Acc. Chem. Res 1999, 32, 975–982;b)Davis AV, Fiedler D, Seeber G, Zahl A, van Eldik R, Raymond KN, J. Am. Chem. Soc 2006, 128, 1324–1333; [PubMed: 16433551] c)Tidmarsh IS, Faust TB, Adams H, Harding LP, Russo L, Clegg W, Ward MD, J. Am. Chem. Soc 2008, 130, 15167–15175; [PubMed: 18855358] d)Cullen W, Metherell AJ, Wragg AB, Taylor CGP, Williams NH, Ward MD, J. Am. Chem. Soc 2018, 140, 2821–2828. [PubMed: 29412665]

[8]. a)Akine S, Miyashita M, Nabeshima T, J. Am. Chem. Soc 2017, 139, 4631–4634; [PubMed: 28291349] b)Wang H, Liu F, Helgeson RC, Houk KN, Angew. Chem., Int. Ed 2013, 52, 655–659;Angew. Chem 2013, 125, 264–268.

[9]. a)Nabeshima T, Yoshihira Y, Saiki T, Akine S, Horn E, J. Am. Chem. Soc 2003, 125, 28–29; [PubMed: 12515495] b)Escobar L, Villarón D, Escudero-Adán EC, Ballester P, Chem. Commun 2019, 55, 604–607.c)Escobar L, Escudero-Adán EC, Ballester P, Angew. Chem., Int. Ed 2019, 58, 16105–16109;Angew. Chem 2019, 131, 16251–16255.

[10]. Zarra S, Smulders MMJ, Lefebvre Q, Clegg JK, Nitschke JR, Angew. Chem., Int. Ed 2012, 51, 6882–6885;Angew. Chem 2012, 124, 6988–6991.

[11]. Bogie PM, Miller TF, Hooley RJ, Isr. J. Chem 2019, 59, 130–139.

[12]. a)Bolliger JL, Belenguer AM, Nitschke JR, Angew. Chem., Int. Ed 2013, 52, 7958–7962;Angew. Chem 2013, 125, 8116–8120;b)Ronson TK; Pilgrim BS; Nitschke JR, J. Am. Chem. Soc 2016, 138, 10417–10420; [PubMed: 27500974] c)Meng W, Clegg JK, Thoburn JD, Nitschke JR, J. Am. Chem. Soc 2011, 133, 13652–13660; [PubMed: 21790184] d)Ronson TK, Meng W, Nitschke JR, J. Am. Chem. Soc 2017, 139, 9698–9707. [PubMed: 28682628]

[13]. a)Holloway LR, Bogie PM, Lyon Y, Ngai C, Miller TF, Julian RR, Hooley RJ, J. Am. Chem. Soc 2018, 140, 8078–8081; [PubMed: 29913069] b)Ngai C, Wu H-T, da Camara B, Williams CG, Mueller LJ, Julian RR, Hooley RJ, Angew. Chem., Int. Ed 2022, 61, e202117011;Angew. Chem 2022, 134, e202117011.

[14]. a)Hristova YR, Smulders MMJ, Clegg JK, Breiner B, Nitschke JR, Chem. Sci 2011, 2, 638–641;b)Bolliger JL, Ronson TK, Ogawa M, Nitschke JR, J. Am. Chem. Soc 2014, 136, 14545–14553; [PubMed: 25226369] c)McConnell AJ, Aitchison CM, Grommet AB, Nitschke JR, J. Am. Chem. Soc 2017, 139, 6294–6297; [PubMed: 28426930] d)Castilla AM, Ronson TK, Nitschke JR, J. Am. Chem. Soc 2016, 138, 2342–2351; [PubMed: 26799196] e)Zhang D, Ronson TK, Mosquera J, Martinez A, Guy L, Nitschke JR, J. Am. Chem. Soc 2017, 139, 6574–6577. [PubMed: 28463507]

[15]. Ferguson A, Staniland RW, Fitchett CM, Squire MA, Williamson BE, Kruger PE, Dalton Trans. 2014, 43, 14550–14553. [PubMed: 25178679]

[16]. Xu L, Zhang D, Ronson TK, Nitschke JR, Angew. Chem., Int. Ed 2020, 59, 7435–7438;Angew. Chem 2020, 132, 7505–7508.

[17]. Rizzuto FJ, Wu W-Y, Ronson TK, Nitschke JR, Angew. Chem., Int. Ed 2016, 55, 7958–7962;Angew. Chem 2016, 128, 8090–8094.

[18]. Geometries optimized with the def2-TZVPPD basis set, and molar volumes calculated in Gaussian.

[19]. Mecozzi S, Rebek J Jr. Chem.-Eur. J 1998, 4, 1016–1022.

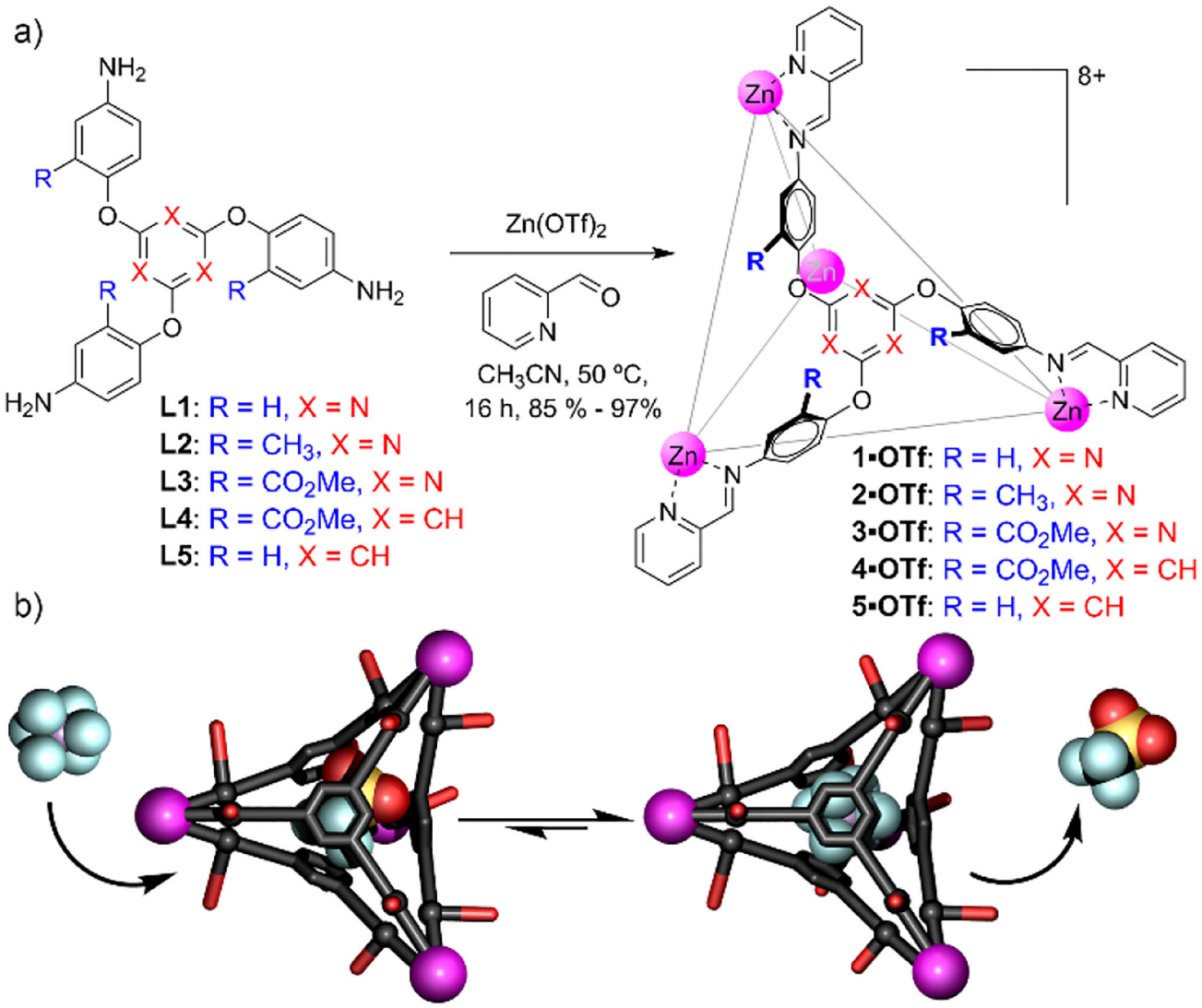

Figure 1.

a) Self-assembled cage complexes tested for selective anion binding. b) Schematic of the anion exchange process.

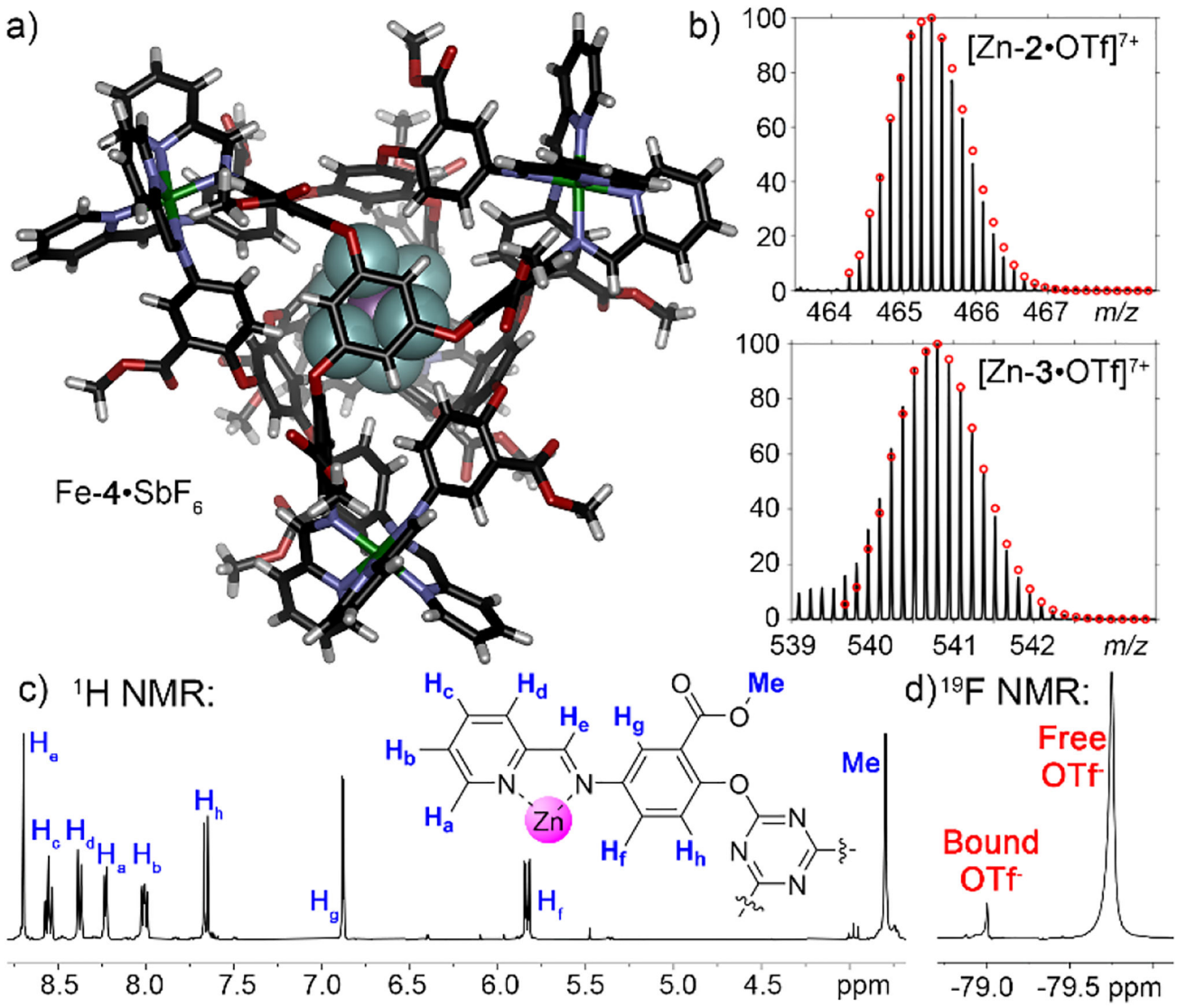

Figure 2. Cage characterization.

a) Molecular structure of the **Fe-4•SbF$_6$** complex, as determined by SCXRD; b) observed isotope patterns for M_4L_4 ions in the ESI-MS spectra of **Zn-2•OTf** and **Zn-3•OTf** (red dots = theoretical peak intensities for the calculated isotope patterns); c) ^{1}H and d) ^{19}F NMR spectra of **Zn-3•OTf** (CD_3CN, 400 MHz, 298 K).

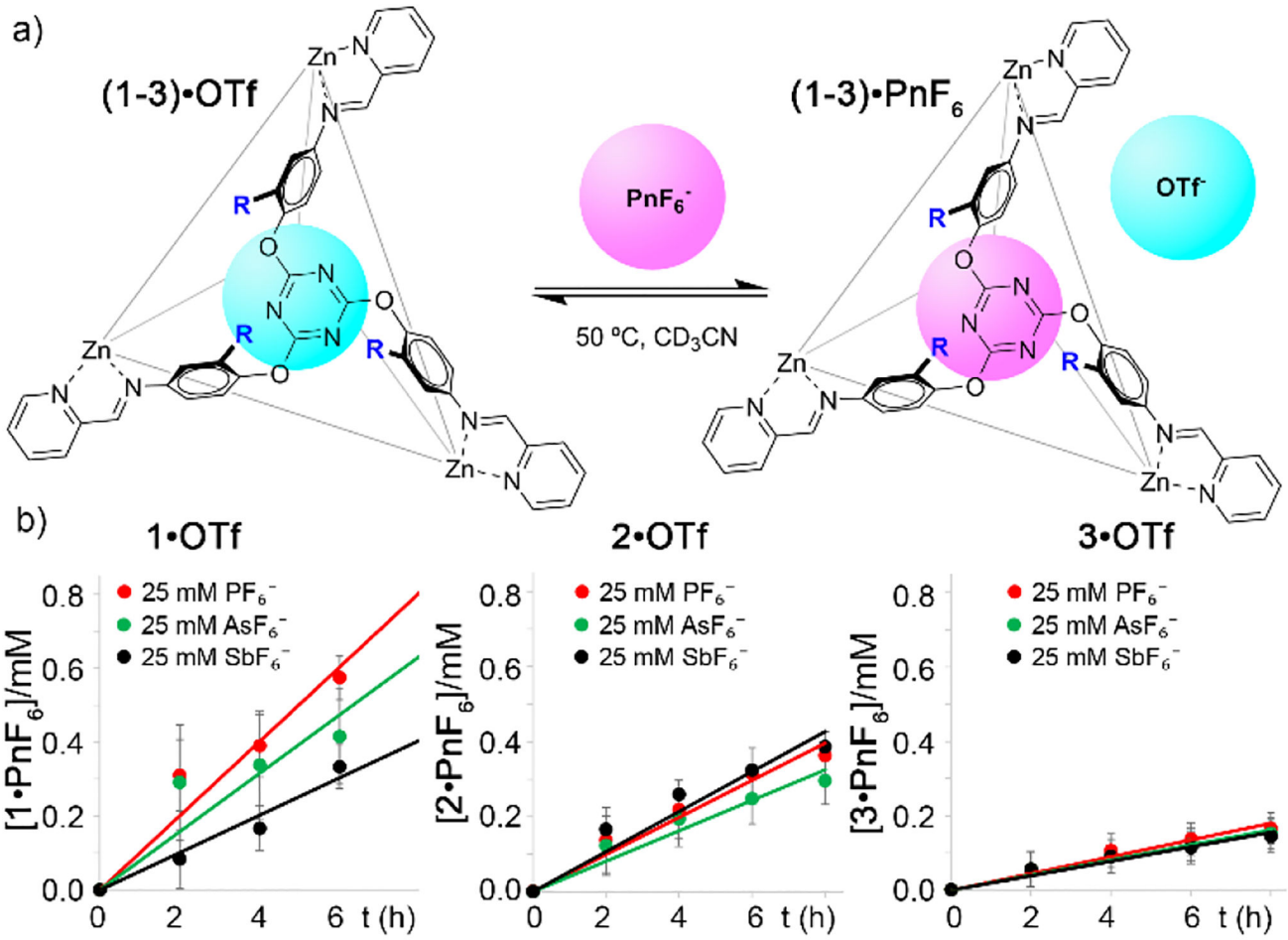

Figure 3. Anion Exchange.

a) Representation of the anion exchange process for **(1–3)•OTf** with various PnF_6^- ions;

b) Initial rate plots of the exchange process, [**1–3**] = 1.0 mM; [PnF_6^-] = 25 mM, CD_3CN, 323K.

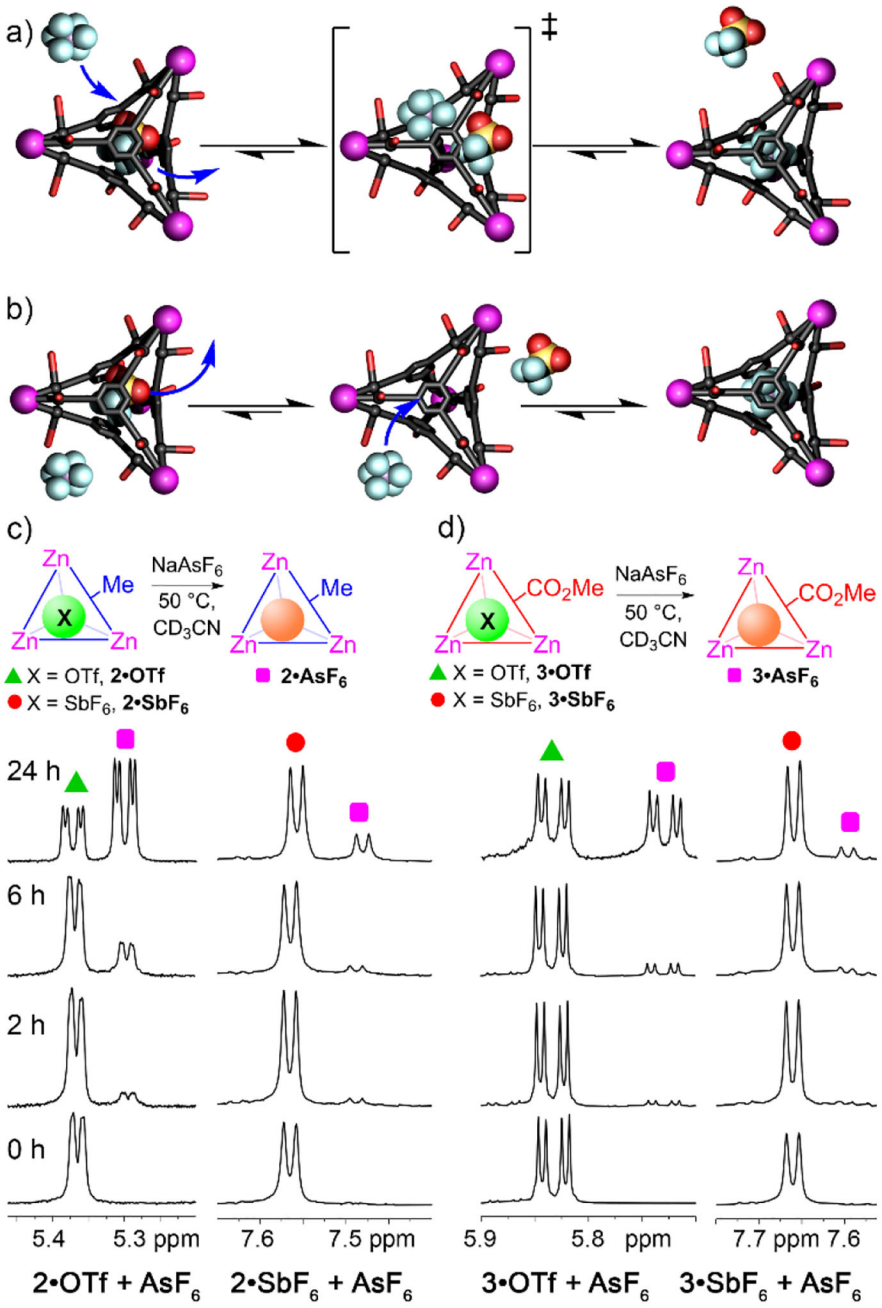

Figure 4. Exchange Mechanisms.

Illustrations of the possible a) associative "S_N2-like" and b) dissociative "S_N1-like" exchange mechanisms. c) Expansions of the ^{1}H NMR spectra showing the difference in exchange rate upon addition of AsF_6^- to cages **2/3•OTf** and **2/3•SbF$_6$** and heating at 50 °C for the noted time (400 MHz, CD_3CN, acquired at 298K).

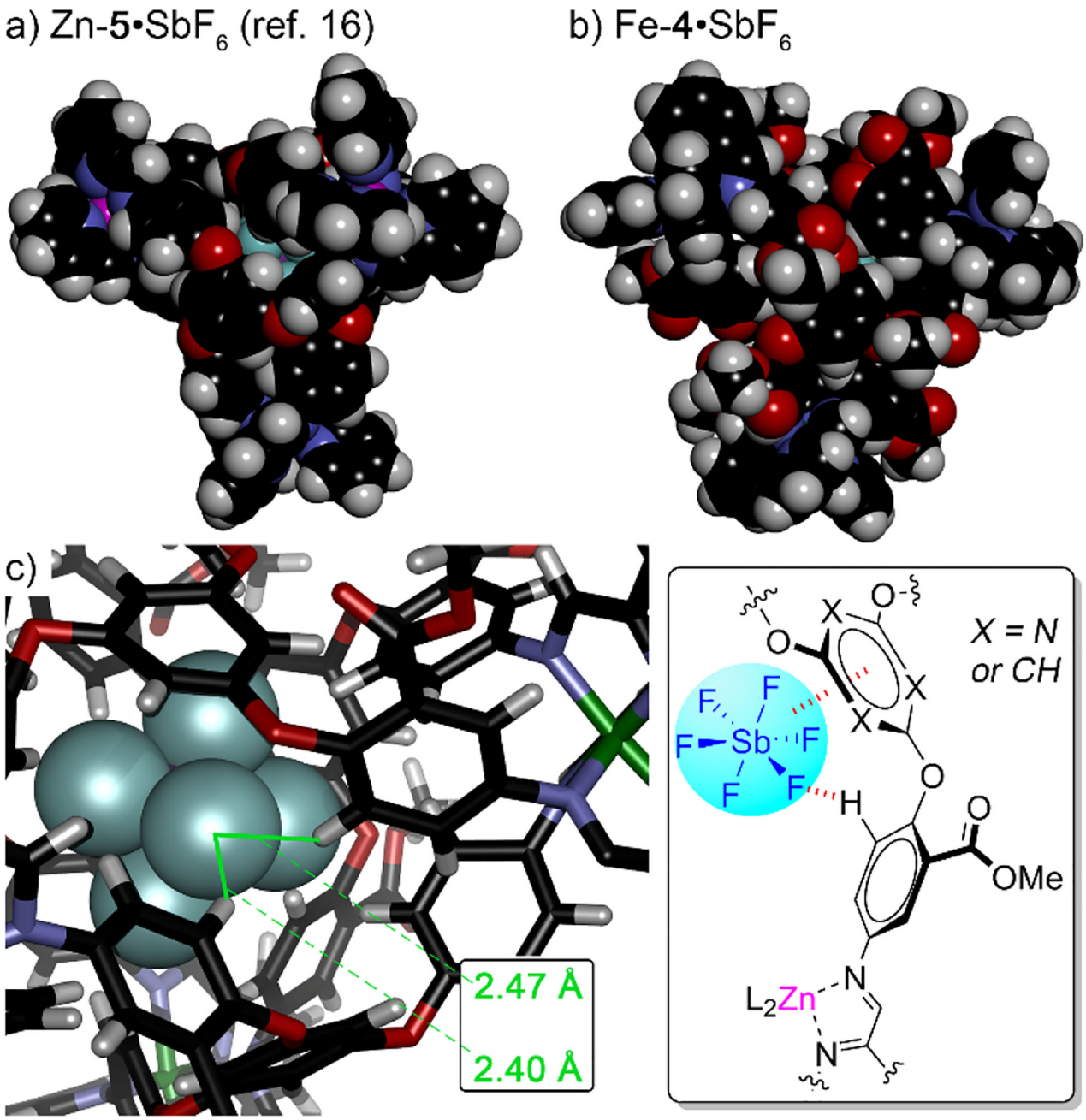

Figure 5. Structural Analysis.

a) Molecular structures as determined by SCXRD of a) **Zn-5•SbF$_6$** (from ref 16) and b) **Fe-4•SbF$_6$**. c) Expansion of the **Fe-4•SbF$_6$**, showing estimated CH-F distances between internal protons H_h and bound anion.

Table 1.

Relative affinities (K_{rel}) of anions in cages (**1–5**)•**OTf**, determined relative to the affinity of OTf^-.[a]

Guest Anion	K_{rel} (1)	K_{rel} (2)	K_{rel} (3)	K_{rel} (4)	K_{rel} (5)[c]
BF_4^-	n.b.[b]	n.b. [b]	n.b. [b]	n.b. [b]	n.b. [b]
PF_6^-	19	20	2.4	0.1	n.d.
AsF_6^-	19	58	38	0.4	1.0
SbF_6^-	~25[d]	25	15	44	5.8

[a] [**1–5**] = 1.0 mM; [anion] = 1.0 mM, CD_3CN, samples heated for 72 h (**1**, **4**, **5**) or 14 days (**2**,**3**) to ensure full equilibration.

[b] no binding seen.

[c] Data reprinted from ref 16.

[d] Estimated K_{rel} (see text).